

# A search for non- $q\bar{q}$ mesons at the CERN Omega Spectrometer

A. Kirk

School of Physics and Astronomy, University of Birmingham, Birmingham, U.K.

## Abstract

The non-Abelian nature of QCD suggests that particles that have a gluon constituent, such as glueballs or hybrids, should exist. Experiments WA76, WA91 and WA102 have performed a dedicated search for these states in central production using the CERN Omega Spectrometer. Several non- $q\bar{q}$  candidates have been observed. This paper presents a study of central meson production as a function of the difference in transverse momentum ( $dP_T$ ) of the exchanged particles which shows that undisputed  $q\bar{q}$  mesons are suppressed at small  $dP_T$  whereas the glueball candidates are enhanced.

**Dedicated to the memory of my colleague and friend Yuri Prokoshkin**

Submitted to Yadernaya Fizika

# 1 Introduction

The present understanding of strong interactions is that they are described by Quantum ChromoDynamics (QCD). This non-Abelian field theory not only describes how quarks and anti-quarks interact, but also predicts that the gluons which are the quanta of the field will themselves interact to form mesons. If the object formed is composed entirely of valence gluons the meson is called a glueball, however if it is composed of a mixture of valence quarks, antiquarks and gluons (i.e.  $q\bar{q}g$ ) it is called a hybrid. In addition,  $q\bar{q}q\bar{q}$  states are also predicted.

The best estimate for the masses of glueballs comes from lattice gauge theory calculations [1] which show that the lightest glueball has  $J^{PC} = 0^{++}$  and that

$$m(2^{++})/m(0^{++}) = 1.5$$

and depending on the extrapolation used from the lattice parameters to mass scale that

$$m(0^{++}) = (1500 - 1750)\text{MeV}.$$

The mass of the  $0^{-+}$  glueball is predicted to be similar to that of the  $2^{++}$  glueball whilst glueballs with other quantum numbers are predicted to be higher in mass.

The flux tube model has been used to calculate the masses of the lowest lying hybrid states and recent predictions [2] are that

$$m(1^{--}, 0^{-+}, 1^{-+}, 2^{-+}) \approx 1900 \text{ MeV}.$$

Hence, these non- $q\bar{q}$  states are predicted to be in the same mass range as the normal  $q\bar{q}$  nonet members and hence we need a method of identifying them.

The following have been suggested as possible ways to identify gluonic states.

- To look for "oddballs": States with  $J^{PC}$  quantum numbers not allowed for normal  $q\bar{q}$  states. For example  $J^{PC} = 1^{-+}$ .
- However the lightest non- $q\bar{q}$  states are predicted to have the same quantum numbers as  $q\bar{q}$  states. Therefore we need to look for extra states, that is states that have quantum numbers of already completed nonets and that have masses which are sufficiently low that they are unlikely to be members of the radially excited nonets and hence they can not be described as being pure  $q\bar{q}$  states.
- If extra states are found then in order to isolate which state is the likely non- $q\bar{q}$  state we can
  - a) Look for states with unusual branching ratios.
  - b) Look for states preferentially produced in gluon rich processes. These processes are described below.

Fig. 1 summarises several dynamical configurations which have been suggested as possible sources of gluonium and where experiments have been performed.

1. Pomeron-Pomeron scattering is shown in fig. 1a). The Pomeron is an object which can be described as a multi-gluon state, and is thought to be responsible for the large cross sections of diffractive reactions. Consequently Double Pomeron Exchange (DPE) is considered to be a possible source of glueballs.
2. The  $J/\psi$  decay is believed to be a highly glue rich channel either via the hadronic decay shown in fig. 1b), or via the radiative decay shown in fig. 1c).
3. Figure 1d) shows proton-antiproton annihilation; the annihilation region of quarks and antiquarks is a source of gluons where glueballs and hybrids could be produced.
4. Special hadronic reactions, an example of which is shown in fig. 1e) where the  $\phi\phi$  system is thought to be produced via an intermediate state containing gluons. Reactions of this kind which have disconnected quark lines are said to be OZI violating [3].

The first reaction is the one studied by experiments WA76, WA91 and WA102 at the Omega spectrometer. In this paper the status of these experiments is reviewed and the possibility of a glueball- $q\bar{q}$  filter in central production is discussed.

## 2 The Omega Central production experiments

There is considerable current interest in trying to isolate the lightest glueball. Several experiments have been performed using glue-rich production mechanisms. One such mechanism is Double Pomeron Exchange (DPE) where the Pomeron is thought to be a multi-gluonic object. Consequently it has been anticipated that production of glueballs may be especially favoured in this process [4].

The Omega central production experiments (WA76, WA91 and WA102) are designed to study exclusive final states formed in the reaction

$$pp \longrightarrow p_f X^0 p_s,$$

where the subscripts  $f$  and  $s$  refer to the fastest and slowest particles in the laboratory frame respectively and  $X^0$  represents the central system. Such reactions are expected to be mediated by double exchange processes where both Pomeron and Reggeon exchange can occur.

The trigger was designed to enhance double exchange processes with respect to single exchange and elastic processes. Details of the trigger conditions, the data processing and event selection have been given in previous publications [5].

## 3 The possibility of a Glueball- $q\bar{q}$ filter in central production

The experiments have been performed at incident beam momenta of 85, 300 and 450 GeV/c, corresponding to centre-of-mass energies of  $\sqrt{s} = 12.7, 23.8$  and 28 GeV. Theoretical predictions

[6] of the evolution of the different exchange mechanisms with centre of mass energy,  $\sqrt{s}$ , suggest that

$$\begin{aligned}\sigma(\text{RR}) &\sim s^{-1}, \\ \sigma(\text{RP}) &\sim s^{-0.5}, \\ \sigma(\text{PP}) &\sim \text{constant},\end{aligned}$$

where RR, RP and PP refer to Reggeon-Reggeon, Reggeon-Pomeron and Pomeron-Pomeron exchange respectively. Hence we expect Double Pomeron Exchange (DPE) to be more significant at high energies, whereas the Reggeon-Reggeon and Reggeon-Pomeron mechanisms will be of decreasing importance. The decrease of the non-DPE cross section with energy can be inferred from data taken by the WA76 collaboration using pp interactions at  $\sqrt{s}$  of 12.7 GeV and 23.8 GeV [7]. The  $\pi^+\pi^-$  mass spectra for the two cases show that the signal-to-background ratio for the  $\rho^0(770)$  is much lower at high energy, and the WA76 collaboration report that the ratio of the  $\rho^0(770)$  cross sections at 23.8 GeV and 12.7 GeV is  $0.44 \pm 0.07$ . Since isospin 1 states such as the  $\rho^0(770)$  cannot be produced by DPE, the decrease of the  $\rho^0(770)$  signal at high  $\sqrt{s}$  is consistent with DPE becoming relatively more important with increasing energy with respect to other exchange processes.

However, even in the case of pure DPE the exchanged particles still have to couple to a final state meson. The coupling of the two exchanged particles can either be by gluon exchange or quark exchange. Assuming the Pomeron is a colour singlet gluonic system if a gluon is exchanged then a gluonic state is produced, whereas if a quark is exchanged then a  $q\bar{q}$  state is produced (see figures 2a) and b) respectively). It has been suggested recently [8] that for small differences in transverse momentum between the two exchanged particles an enhancement in the production of glueballs relative to  $q\bar{q}$  states may occur.

Recently the WA91 collaboration has published a paper [9] showing that the observed centrally produced resonances depend on the angle between the outgoing slow and fast protons. In order to describe the data in terms of a physical model, Close and Kirk [8] have proposed that the data be analysed in terms of the difference in transverse momentum between the particles exchanged from the fast and slow vertices.

The trigger is described in detail in ref. [9]. In brief, the trigger separates the data into two categories. One where the slow and fast particles are on the same side of the beam, *i.e.* a small azimuthal angle between the outgoing protons (classified as LL) and one where the slow and fast particles are on the opposite side of the beam, *i.e.* the azimuthal angle between the outgoing protons is near to 180 degrees, (classified as LR).

In ref. [9] it was shown that the centrally produced resonances depended on the trigger type *i.e.* the resonances observed in the LL trigger were different to those observed in the LR trigger. This difference was not due to any acceptance or trigger bias but appeared to be related to the angle between the outgoing protons. Figures 2c) and d) show schematic representations of the LL and LR triggers respectively in the centre of mass of the beam plus target where the longitudinal (x) axis is defined to be along the beam direction. In the case of the LL trigger (figure 2c)) the transverse momentum vector of each exchanged particle has the same sign whereas for the LR trigger (figure 2d)) they have the opposite sign. Hence the difference in the transverse momentum vectors of the two exchanged particles is greater in the LR trigger than in the LL trigger. The difference in the transverse momentum vectors ( $dP_T$ ) is defined to be

$$dP_T = \sqrt{(P_{y1} - P_{y2})^2 + (P_{z1} - P_{z2})^2}$$

where  $P_{y_i}$ ,  $P_{z_i}$  are the y and z components of the momentum of the  $i$ th exchanged particle in the pp centre of mass system.

Figures 3a) and b) show the  $dP_T$  spectrum for the LL and LR trigger types respectively. As can be seen the LL trigger type have access to events with smaller  $dP_T$ . It has been shown by Monte Carlo simulation that this effect is not due to the fact that the LR events have additional trigger requirements but it is due only to the fact that the two protons recoil on the same (LL) or opposite (LR) side of the beam direction [9].

The effect that different cuts in  $dP_T$  have on the  $\pi^+\pi^-$  mass spectrum are shown in figures 3c), d) and e). As can be seen, for  $dP_T < 0.2$  GeV there is effectively no  $\rho^0(770)$  or  $f_2(1270)$  signals. These signals only become apparent as  $dP_T$  increases. However the  $f_0(980)$ , which is responsible for the sharp drop in the spectrum around 1 GeV, is clearly visible in the small  $dP_T$  sample.

Figures 4a), b) and c) show the effect of the  $dP_T$  cut on the  $K^+K^-$  mass spectrum where structures can be observed in the 1.5 and 1.7 GeV mass region which have been previously identified as the  $f_2'(1525)$  and the  $f_J(1710)$  [10]. As can be seen, the  $f_2'(1525)$  is produced dominantly at high  $dP_T$ , whereas the  $f_J(1710)$  is produced dominantly at low  $dP_T$ .

In the  $\pi^+\pi^-\pi^+\pi^-$  mass spectrum a dramatic effect is observed, see figures 4d), e) and f). The  $f_1(1285)$  signal has virtually disappeared at low  $dP_T$  whereas the  $f_0(1500)$  and  $f_2(1900)$  signals remain.

A spin-parity analysis of the  $\pi^+\pi^-\pi^+\pi^-$  channel has been performed [11] using an isobar model [12]. The  $f_1(1285)$  is clearly seen in the  $J^P = 1^+ \rho\rho$  and the  $f_1(1285)$  signal almost disappears at small  $dP_T$ . In the  $J^P = 0^+ \rho\rho$  distribution a peak is observed at 1.45 GeV together with a broad enhancement around 2 GeV. The peak in the  $J^P = 0^+ \rho\rho$  wave around 1.45 GeV remains for  $dP_T \leq 0.2$  GeV while the  $J^P = 0^+$  enhancement at 2.0 GeV becomes less important: which shows that the  $dP_T$  effect is not simply a  $J^P$  filter.

A fit has first been performed to the total  $J^P = 0^+ \rho\rho$  distribution using a K matrix formalism [13] including poles to describe the peak at 1.45 GeV as an interference between the  $f_0(1300)$ , the  $f_0(1500)$  together with a possible state at 2 GeV. The resulting resonance parameters for the  $f_0(1300)$  and  $f_0(1500)$  are very similar to those found by Crystal Barrel [14].

The peak observed at 1.9 GeV, called the  $f_2(1900)$ , is found to decay to  $a_2(1320)\pi$  and  $f_2(1270)\pi\pi$  with  $J^{PC} = 2^{++}$ . At small  $dP_T$  the  $f_2(1900)$  signal is still important. This is the first evidence of a non-zero spin resonance produced at small  $dP_T$  and hence shows that the  $dP_T$  effect is not just a  $J^P = 0^+$  filter.

In addition to these waves, a  $J^P = 2^- a_2(1320)\pi$  wave was required in the fit. The  $J^P = 2^- a_2(1320)\pi$  wave observed in this experiment is consistent with the two  $\eta_2$  resonances observed by Crystal Barrel [15] with both states decaying to  $a_2(1320)\pi$ . The  $2^- a_2(1320)\pi$  signal is suppressed at small  $dP_T$ . This behaviour is consistent with the signals being due to standard  $q\bar{q}$  states [8].

Similar effects are observed in all the other channels analysed to date [16, 17]. In fact it has been observed that all the undisputed  $q\bar{q}$  states (i.e.  $\rho^0(770)$ ,  $\eta'$ ,  $f_2(1270)$ ,  $f_1(1285)$ ,  $f_2'(1525)$  etc.) are suppressed as  $dP_T$  goes to zero, whereas the glueball candidates  $f_J(1710)$ ,  $f_0(1500)$  and  $f_2(1900)$  survive. It is also interesting to note that the enigmatic  $f_0(980)$ , a possible non- $q\bar{q}$  meson or  $K\bar{K}$  molecule state does not behave as a normal  $q\bar{q}$  state.

A Monte Carlo simulation of the trigger, detector acceptances and reconstruction program shows that there is very little difference in the acceptance as a function of  $dP_T$  in the different mass intervals considered within a given channel and hence the observed differences in resonance production can not be explained as acceptance effects.

It has previously been observed that the resonances produced in the central region depend on the four momentum transferred from the fast ( $t_f$ ) and slow vertices ( $t_s$ ) [7]. The  $\pi^+\pi^-$  mass spectrum is shown for the case where  $|t_f|$  and  $|t_s|$  are both less than  $0.15 \text{ GeV}^2$  in figure 5a) and in figure 5b) for the case when  $|t_f|$  and  $|t_s|$  are both greater than  $0.15 \text{ GeV}^2$ . As can be seen the amount of  $\rho^0(770)$  and  $f_2(1270)$  does change as a function of this cut. In figures 5c) and d) the  $dP_T$  distribution for these two cases is shown. As can be seen the events that have small  $|t|$  are restricted to small values of  $dP_T$ . To show that  $dP_T$  is the most important underlying dynamical effect the  $dP_T$  cut has been applied to the sample of events with large  $|t|$ . Figures 5e), f) and g) show the events when  $|t_f|$  and  $|t_s|$  are both greater than  $0.15 \text{ GeV}^2$  for  $dP_T \leq 0.2 \text{ GeV}$ ,  $0.2 \leq dP_T \leq 0.5 \text{ GeV}$  and  $dP_T \geq 0.5 \text{ GeV}$  respectively. As can be seen the  $dP_T$  cut still works in this sample.

## 4 Summary of the effects of the $dP_T$ filter

In order to calculate the contribution of each resonance as a function of  $dP_T$  the acceptance corrected mass spectra have been fitted with the parameters of the resonances fixed to those obtained from the fits to the total data. The results of these fits are summarised in table 1 where the percentage of each resonance as a function of  $dP_T$  is presented. Some of these values differ from previously published values [11, 16] due to an improved understanding and simulation of the experimental trigger. Figure 6 shows the ratio of the number of events for  $dP_T < 0.2 \text{ GeV}$  to the number of events for  $dP_T > 0.5 \text{ GeV}$  for each resonance considered. It can be observed that all the undisputed  $q\bar{q}$  states which can be produced in DPE, namely those with positive G parity and  $I = 0$ , have a very small value for this ratio ( $\leq 0.1$ ). Some of the states with  $I = 1$  or G parity negative, which can not be produced by DPE, have a slightly higher value ( $\approx 0.25$ ). However, all of these states are suppressed relative to the interesting states, which could have a gluonic component, which have a large value for this ratio.

## 5 Conclusions

The results presented in this paper indicate the possibility of a glueball- $q\bar{q}$  filter mechanism in central production. All the undisputed  $q\bar{q}$  states are observed to be suppressed at small  $dP_T$ , but the glueball candidates  $f_0(1500)$ ,  $f_J(1710)$ , and  $f_2(1900)$ , together with the enigmatic  $f_0(980)$ , survive.

## References

- [1] G. Bali et al. (UKQCD), Phys. Lett. **B309** (1993) 378;  
D. Weingarten, hep-lat/9608070;  
J. Sexton et al., Phys. Rev. Lett. **75** (1995) 4563;  
F.E. Close and M.J. Teper, “On the lightest Scalar Glueball” Rutherford Appleton Laboratory report no. RAL-96-040; Oxford University report no. OUTP-96-35P
- [2] N. Isgur, AIP. Conf. Proc. 185, Particles and Fields 36, Glueballs, hybrids and exotic hadrons, (1988) 3
- [3] S. Okuba, Phys. Lett. **5** (1963) 165;  
G. Zweig, CERN/TH 401,402,412 (1964);  
J. Iizuka, Prog. Theor. Phys. Suppl. **37-38** (1966) 21.
- [4] D. Robson, Nucl Phys **B130** (1977) 328;  
F.E. Close, Rep. Prog. Phys. **51** (1988) 833.
- [5] T.A. Armstrong *et al.*, Nucl. Instr. and Methods **A274** (1989) 165;  
F. Antinori *et al.*, Il Nuovo Cimento **A107** (1994) 1857.
- [6] S.N. Ganguli and D.P. Roy, Phys. Rep. **67** (1980) 203.
- [7] T.A. Armstrong et al., Zeit. Phys. **C 51** (1991) 351.
- [8] F.E. Close and A. Kirk, Phys. Lett. **B397** (1997) 333.
- [9] D. Barberis et al., Phys. Lett. **B388** (1996) 853.
- [10] T.A. Armstrong et al., Phys. Lett. **B227** (1989) 186.
- [11] D. Barberis *et al.*, Phys. Lett. **B413** (1997) 217.
- [12] S. Abatzis *et al.*, Phys. Lett. **B324** (1994) 509.
- [13] S.U. Chung *et al.*, Ann. d. Physik. **4** (1995) 404.
- [14] A. Abele *et al.*, Nucl. Phys. **A609** (1996) 562.
- [15] C. Amsler *et al.*, Zeit. Phys. **C71** (1996) 227.
- [16] D. Barberis *et al.*, Phys. Lett. **B413** (1997) 225.
- [17] D. Barberis *et al.*, hep-ex/9801003, Submitted to Phys. Lett.

Table 1: Resonance production as a function of  $dP_T$  expressed as a percentage of its total contribution. The error quoted represents the statistical and systematic errors summed in quadrature.

$J^{PC}$	Resonance	$dP_T \leq 0.2$ GeV	$0.2 \leq dP_T \leq 0.5$ GeV	$dP_T \geq 0.5$ GeV
$0^{-+}$	$\pi^0$	$12 \pm 2$	$44 \pm 2$	$44 \pm 2$
	$\eta$	$6 \pm 2$	$34 \pm 2$	$60 \pm 3$
	$\eta'$	$3 \pm 2$	$32 \pm 2$	$64 \pm 3$
$0^{++}$	$a_0(980)$	$14 \pm 4$	$35 \pm 4$	$51 \pm 7$
	$f_0(980)$	$22 \pm 2$	$56 \pm 3$	$22 \pm 3$
	$f_0(1300)$	$20 \pm 2$	$48 \pm 2$	$32 \pm 4$
	$f_0(1500)$	$23 \pm 2$	$53 \pm 3$	$24 \pm 4$
	$f_0(2000)$	$5 \pm 3$	$43 \pm 5$	$52 \pm 5$
$1^{++}$	$a_1(1260)$	$13 \pm 3$	$51 \pm 4$	$36 \pm 3$
	$f_1(1285)$	$3 \pm 1$	$35 \pm 2$	$61 \pm 4$
	$f_1(1420)$	$2 \pm 2$	$38 \pm 2$	$60 \pm 4$
$1^{--}$	$\rho(770)$	$8 \pm 2$	$38 \pm 2$	$54 \pm 3$
	$\omega(782)$	$10 \pm 2$	$40 \pm 2$	$49 \pm 3$
	$\phi(1020)$	$10 \pm 3$	$48 \pm 3$	$42 \pm 4$
$2^{-+}$	$\pi_2(1670)$	$11 \pm 2$	$48 \pm 4$	$40 \pm 4$
	$\eta_2(1620)$	$2 \pm 1$	$42 \pm 6$	$54 \pm 5$
	$\eta_2(1875)$	$1 \pm 1$	$36 \pm 7$	$63 \pm 7$
$2^{++}$	$a_2(1320)$	$4 \pm 4$	$35 \pm 3$	$61 \pm 5$
	$f_2(1270)$	$4 \pm 2$	$25 \pm 2$	$71 \pm 3$
	$f_2'(1520)$	$11 \pm 3$	$37 \pm 3$	$52 \pm 4$
	$f_J'(1710)$	$26 \pm 3$	$45 \pm 2$	$29 \pm 4$
	$f_2(1900)$	$26 \pm 2$	$46 \pm 3$	$28 \pm 4$



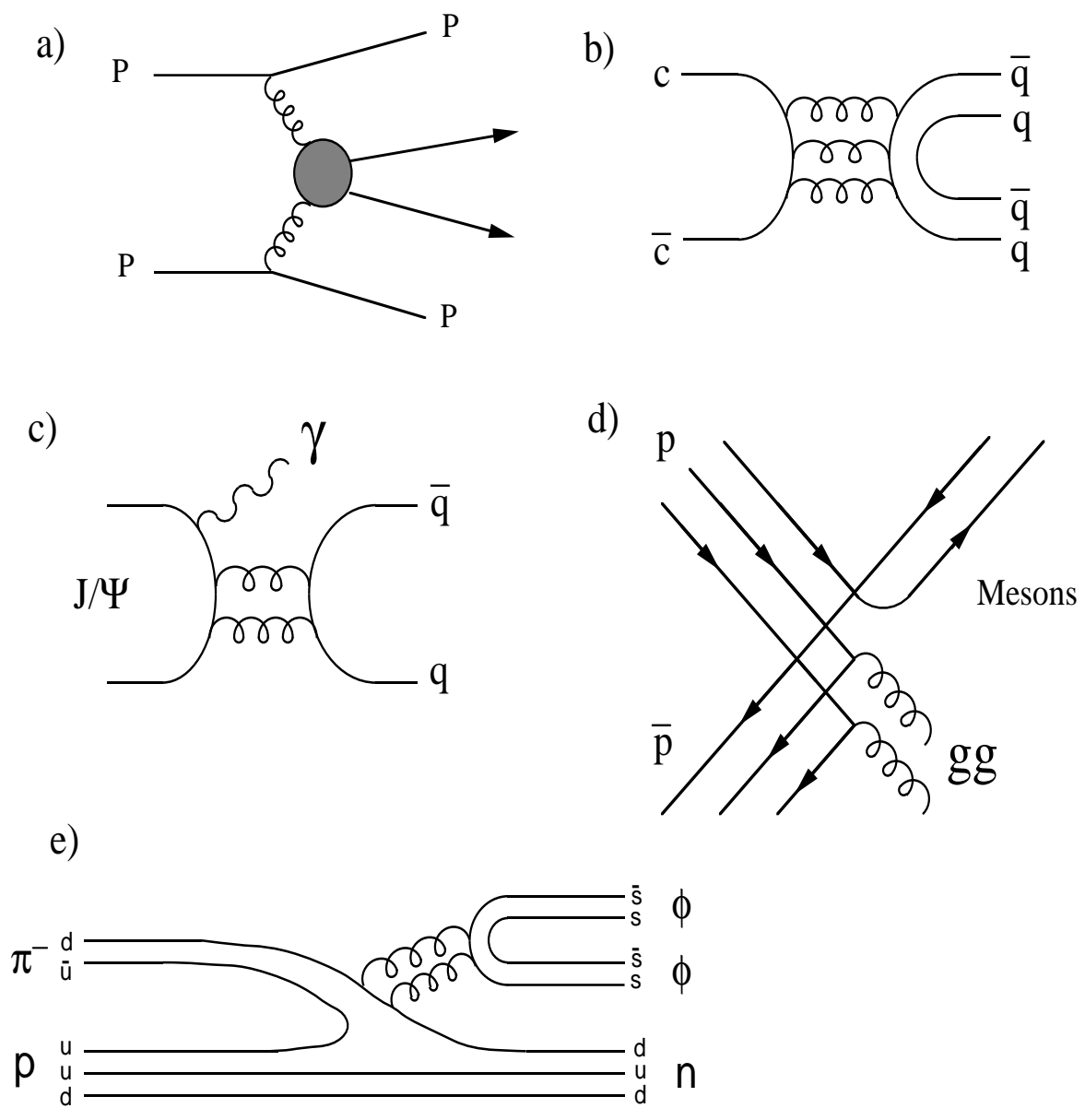


Figure 1: Gluon rich channels. Dynamical configurations that have been used to study light hadron spectroscopy in a search for glueball states.

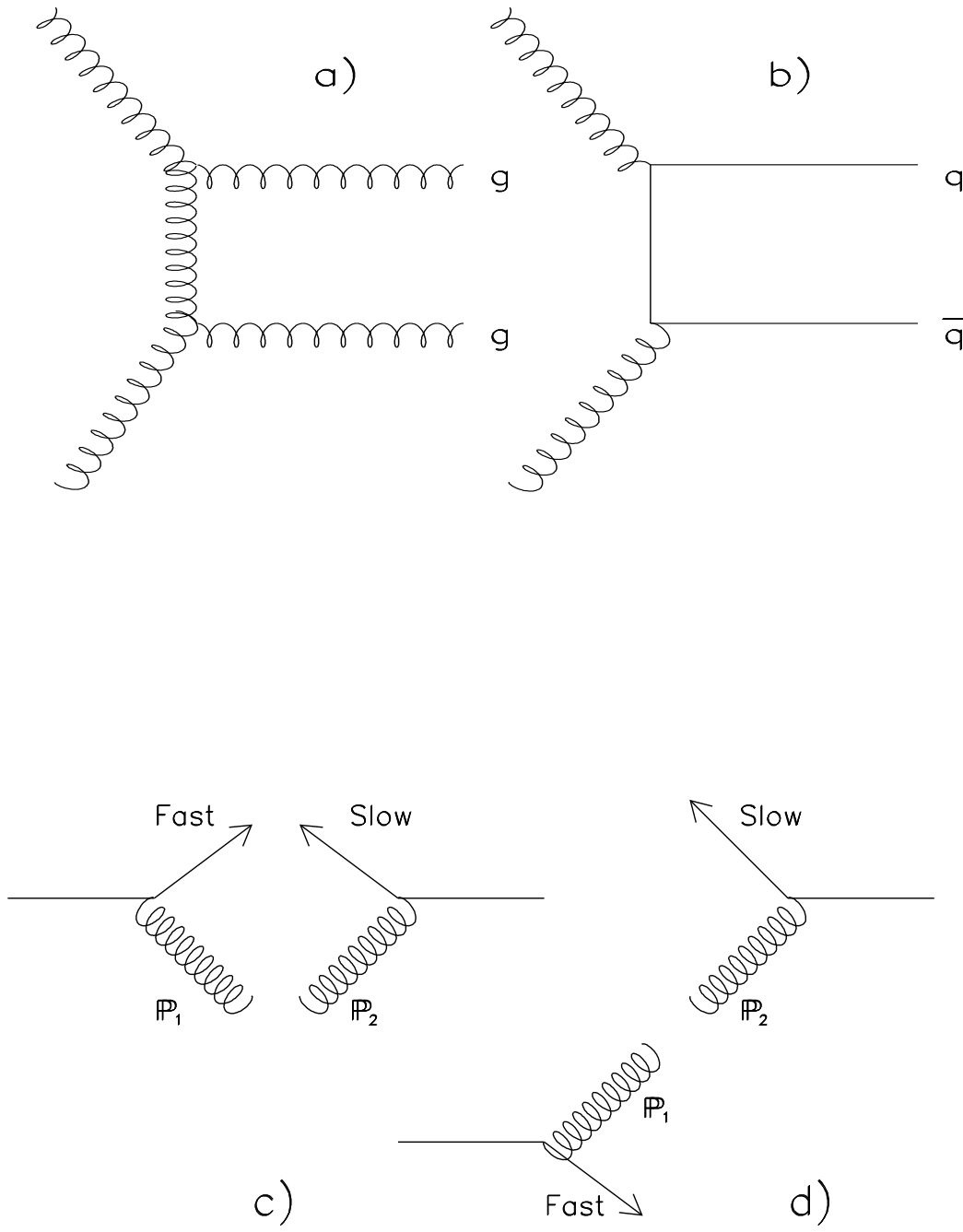


Figure 2: Schematic diagrams of the coupling of the exchange particles into the final state meson for a) gluon exchange and b) quark exchange. Schematic diagrams in the CM for c) LL and d) LR triggers.

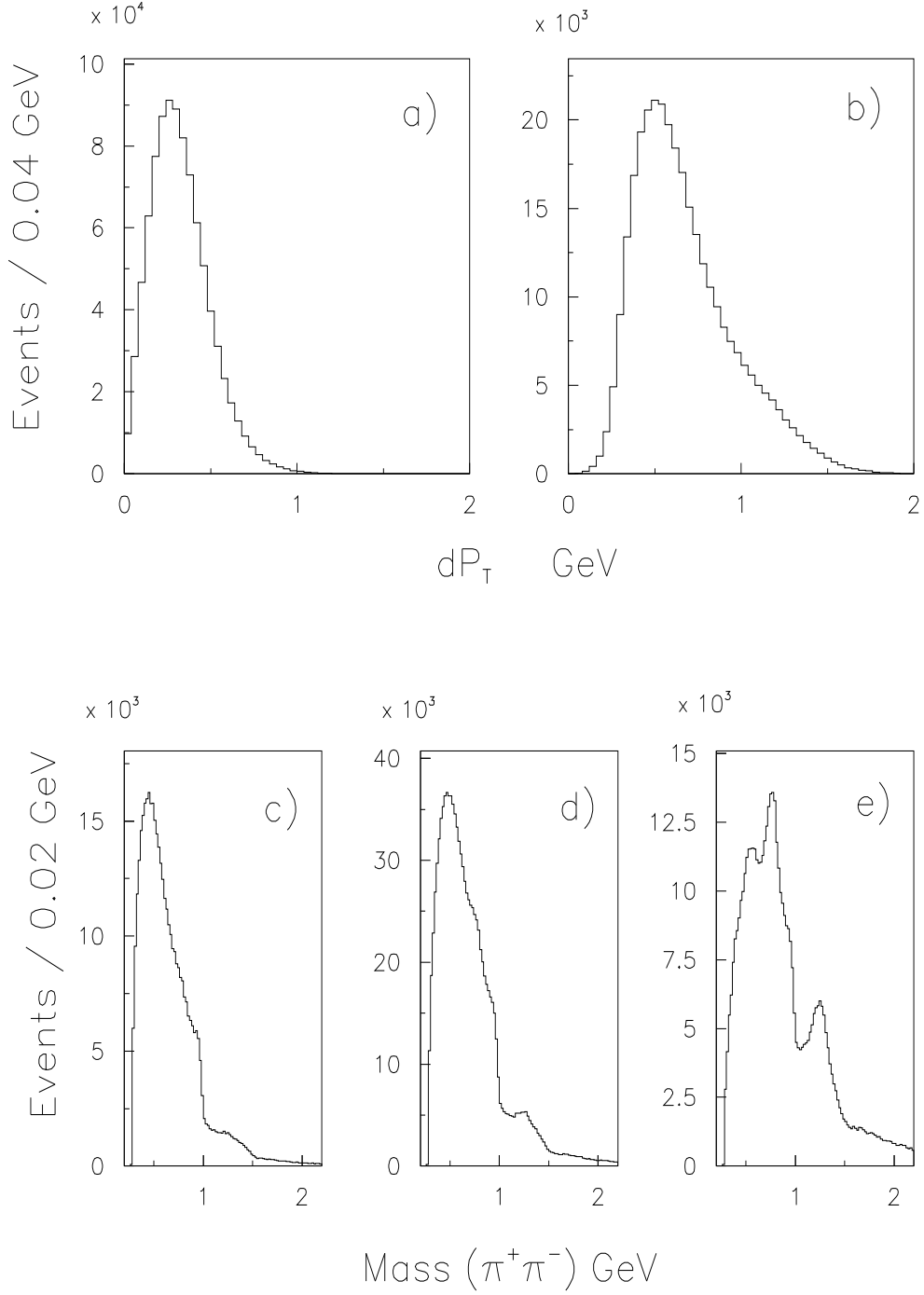


Figure 3:  $dP_T$  for a) LL and b) LR triggered events. The  $\pi^+\pi^-$  mass spectrum for c)  $dP_T < 0.2$  GeV, d)  $0.2 < dP_T < 0.5$  GeV and e)  $dP_T > 0.5$  GeV.

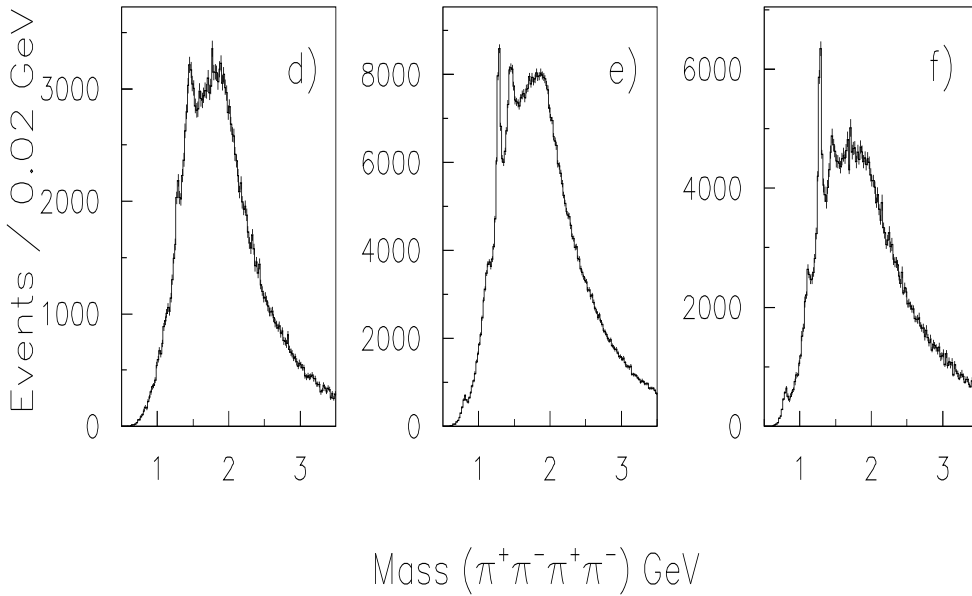
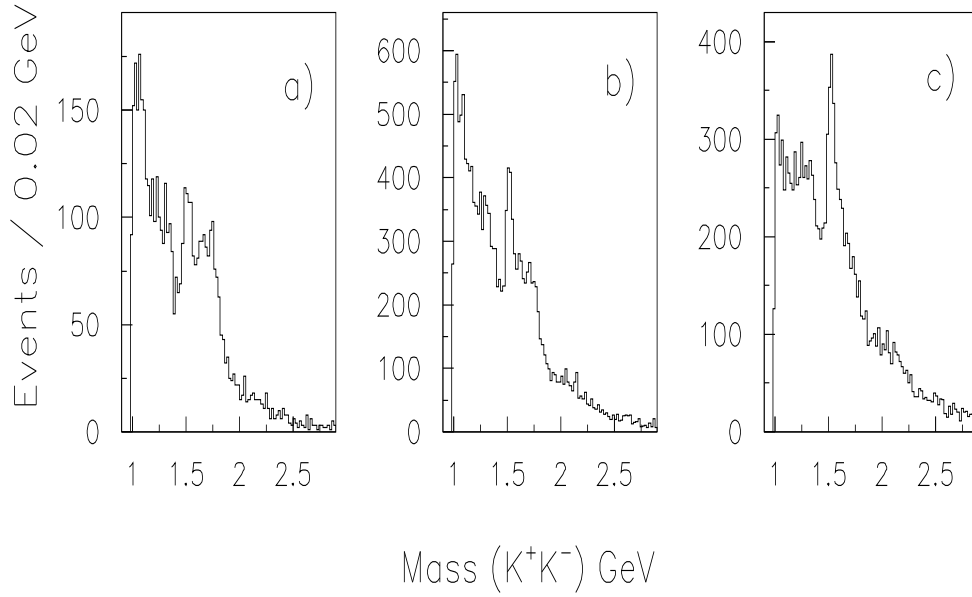


Figure 4:  $K^+K^-$  mass spectrum for a)  $dP_T < 0.2$  GeV, b)  $0.2 < dP_T < 0.5$  GeV and c)  $dP_T > 0.5$  GeV and the  $\pi^+\pi^-\pi^+\pi^-$  mass spectrum for d)  $dP_T < 0.2$  GeV, e)  $0.2 < dP_T < 0.5$  GeV and f)  $dP_T > 0.5$  GeV.

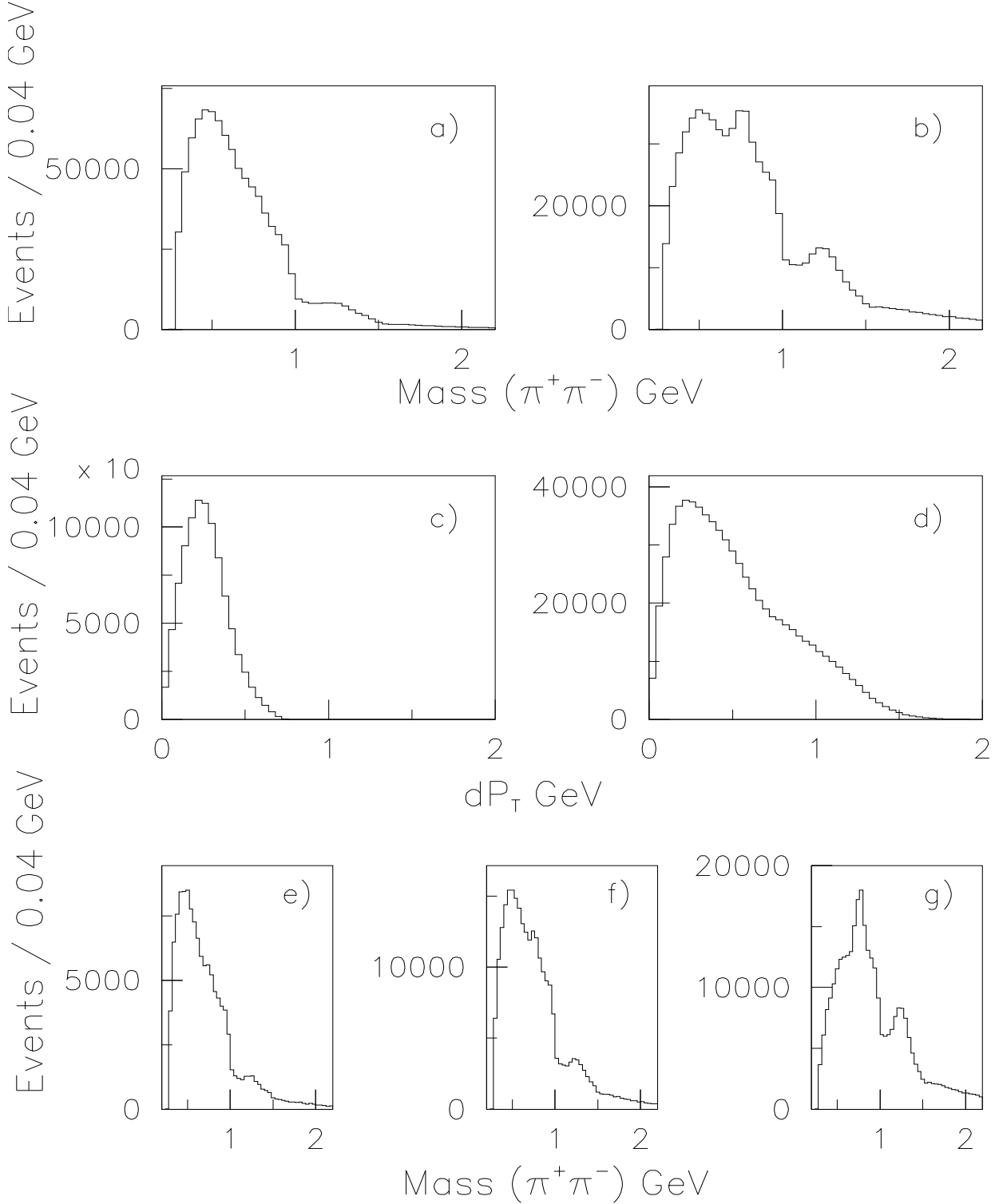


Figure 5: Results of cutting on the four momentum transferred at the proton vertices. The  $\pi^+\pi^-$  mass spectrum for a)  $|t_f| < 0.15$  and  $|t_s| < 0.15$   $\text{GeV}^2$  and b)  $|t_f| > 0.15$  and  $|t_s| > 0.15$   $\text{GeV}^2$ . The  $dP_T$  distribution for c)  $|t_f| < 0.15$  and  $|t_s| < 0.15$   $\text{GeV}^2$  and d)  $|t_f| > 0.15$  and  $|t_s| > 0.15$   $\text{GeV}^2$ . The  $\pi^+\pi^-$  mass spectrum for  $|t_f| > 0.15$  and  $|t_s| > 0.15$   $\text{GeV}^2$  and e)  $dP_T < 0.2$   $\text{GeV}$ , f)  $0.2 < dP_T < 0.5$   $\text{GeV}$  and g)  $dP_T > 0.5$   $\text{GeV}$ .

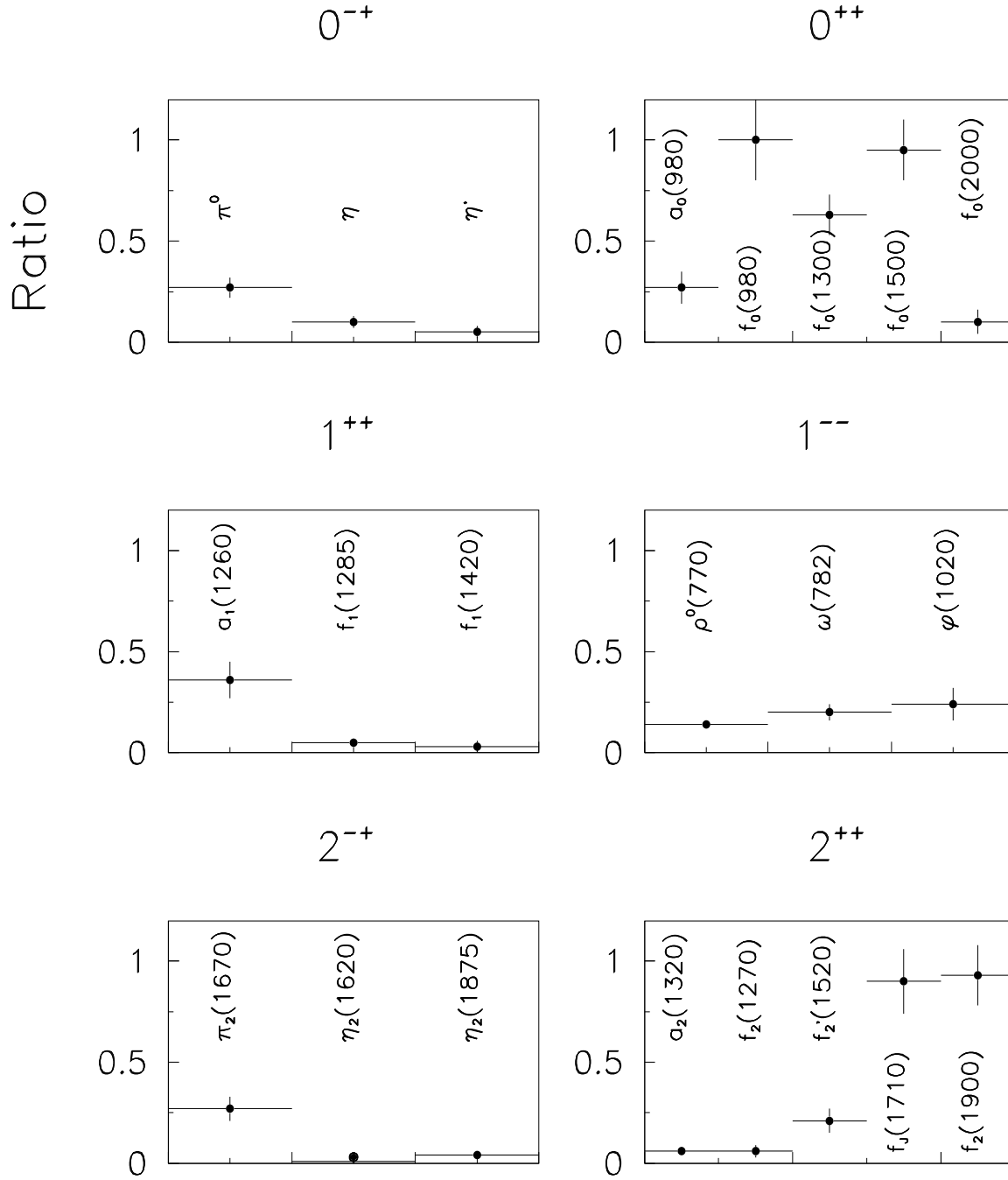


Figure 6: The ratio of the amount of resonance with  $dP_T \leq 0.2$  to the amount with  $dP_T \geq 0.5$  GeV.